Journal of Tissues and Materials

Crystallographic study of hydrothermal synthesis of Hydroxyapatite nano-rods using Brushite precursors

Hassan Nosrati *[1], Rasoul Sarraf Mamoory *[1], Fatemeh Dabir [2]

[1]Department of Materials Engineering, Tarbiat Modares University, Tehran, Iran
[2] Non-metallic Materials Group, Niroo Research Institute, Tehran, Iran
Correspondence to: Nosrati H. (h.nosrati@modares.ac.ir), Sarraf Mamoory R. (rsarrafm@modares.ac.ir)

Abstract

Introduction: Being known for an array of properties that favor hard tissue regeneration, ranging from osteoconductivity to biocompatibility to non-immunogenicity, and being the natural bone mineral phase hydroxyapatite (HA, $Ca_{10}(PO_4)_6(OH)_2$) is the natural bioceramic of choice for the reinforcement phase of biocomposites.

Objective: The main objective of this study is to successfully synthesize uniform one dimensional HA nano-structures using a gram-scale hydrothermal batch process.

Material and Methods: Brushite used as a precursor for HA synthesis. The powders obtained after washing and drying were evaluated. The analysis performed in the sample includes inductively coupled plasma (ICP), Raman Spectroscopy, Fourier transform infrared spectroscopy (FTIR), X-ray diffraction, Field Emission Scanning Electron Microscope (FE-SEM), and high-resolution TEM.

Result: The results of this study showed that the initial brushite used in the hydrothermal process was dissolved, followed by the nucleation process and the growth of hydroxyapatite. The synthesized powders in this study were rod-shaped, with 35 nm in diameter and between 50 and 250 nm in length. The main direction of rod growth was <002>, which is C axis.

Conclusion: The powders synthesized in this research have the potential to be used in bone tissue engineering, implantation, and drug delivery.

Keywords: Hard Tissue Engineering; Hydroxyapatite; Nano-Rods; Hydrothermal

Received: 17 August 2019, Accepted: 10 September 2019

DOI: 10.22034/jtm.2019.199830.1022

1. Introduction

Future biocomposites in bone tissue engineering are probably composed of natural biopolymers as the porous matrix phase and the organic or inorganic phase or hybrid in nano and micro size as reinforcements [1-5]. Being known for an array of properties that favor hard tissue regeneration, ranging from osteoconductivity to biocompatibility to non-immunogenicity, and being the natural bone mineral phase hydroxyapatite (HA, $Ca_{10}(PO_4)_6(OH)_2$) is the natural bioceramic of choice for the reinforcement phase of biocomposites, rivaled in response only by a handful of other materials, such as chitin [6],

bioactive glass [7], carbon nanostructures (graphene, carbone nanotube) [8,9], and others.

Recently, there has been a growing interest in bone tissue engineering for HA nanoparticles and nanostructures with large surface-to-volume ratios [10].

The osteoinductive properties of the materials containing these nanostructures are directly related to their specific surface area [11], which is also very useful for drug delivery. One-dimensional nano and micro-particles such as rods [12-14], wires [15], tubes [16, 17], ribbons [18] and similar morphological porous assembled 3D materials made of them are particularly capable of meeting biomedical applications. The combined effects of nanosized and micro surfaces on the size of the one dimensional material can not only be optimal for cell proliferation and bone differentiation, but also useful for expressing angiogenic factors in stem cell differentiation [19]. The development of controlled synthesis methods for one-dimensional HA nanostructures is largely accomplished by this objective, especially since recent advances in the field have not yet fully met the criteria for effective size and shape control.

The first objective of this study is to successfully synthesize uniform one dimensional HA structures, ranging from nanorods to more complex morphological species, using a gram-scale hydrothermal batch process. The synthesis framework applied by studying traditional hydrothermal and hot solution methods for the synthesis of one dimensional HA structures such as ribbons, whiskers, platelets and tubes [20-24] and organic modifiers assisted methods [25-27]. Brushite (Dicalcium Phosphate Dehydrate), a member of the calcium phosphate family, was used in this study as synthesis precursors. Crystal structure modeling and growth planes for brushite and hydroxyapatite crystals have been performed for ease of understanding the process. The results of this study can be useful for a variety of medical applications, including hard bone tissue engineering, drug delivery and implantation.

2. Materials and Methods

The chemicals used in this study include Calcium nitrate tetrahydrate, Diammonium hydrogenphosphate, and brushite. The properties of these materials have already been published [28]. The brushite used in this study was prepared using the same precipitation method.

In the precipitation stage, the ratio of calcium to phosphate is considered to be 1.67, which is equivalent to that of hydroxyapatite. The precipitation step was carried out inside the Teflon container and after adjusting pH> 10, it was transferred to a hydrothermal autoclave. The hydrothermal process was carried out at 180 ° C for 6 hours. Figure 1 schematically shows the hydrothermal autoclave and Teflon container.

The characterization performed consists of X-ray diffraction (XRD, X' Pert Pro, Panalytical Co.), Fourier transform infrared spectroscopy (FTIR, VERTEX 70, Brucker Co.), Micro-Raman spectroscopy (Reinshaw invia spectrometer), Field Emission Scanning Electron Microscope (FESEM, Hitachi S4700 equipped with energy dispersive X-ray spectroscopy), HRTEM (TALOS F200A), Transmittance Electron Microscopy (TEM, CM120, Philips), and inductively coupled plasma (ICP) (DV7300, Optima Co.). Details of the devices and methods have been published in previous articles [28-30]. The software used in this research includes SolidWorks, Diamond, and ImageJ.

Figure 1: Teflon container (a) and hydrothermal autoclave (b)

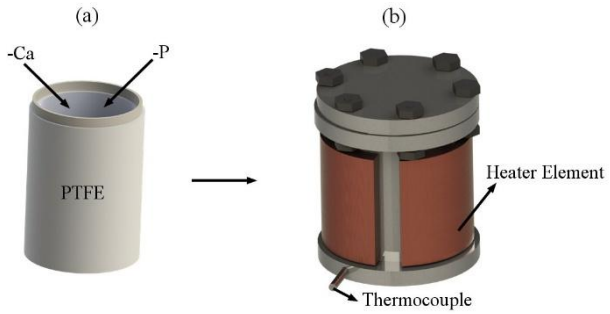

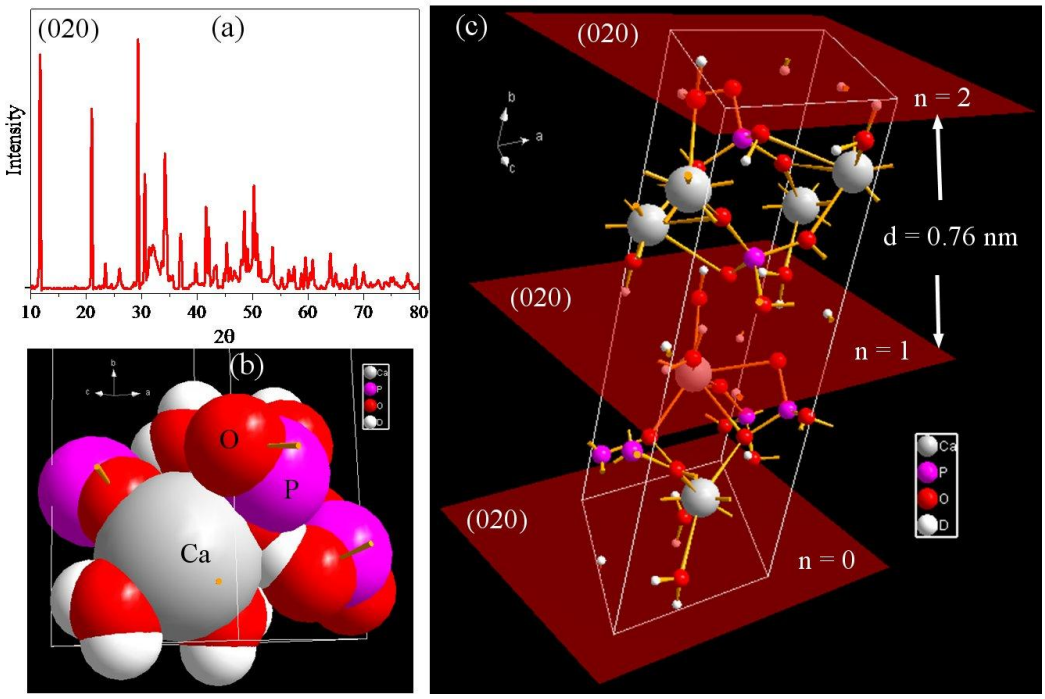

Figure 2: XRD analysis (a), schematic image of brushite unit cell (b), and crystal growth planes of brushite (c).

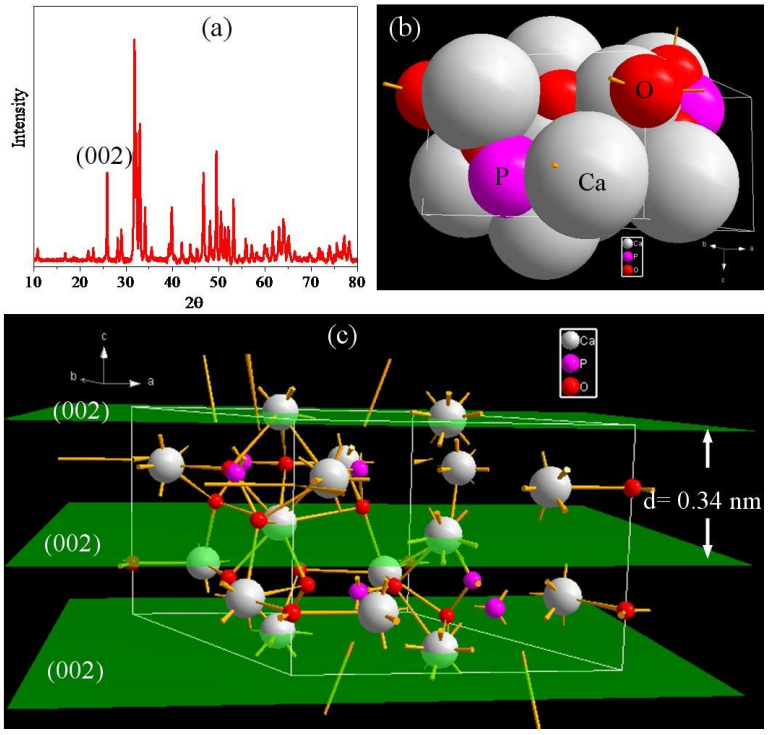

Figure 3: XRD analysis (a), schematic image of hydroxyapatite unit cell (b), and crystal growth planes of hydroxyapatite (c).

3. Results and Discussion

Figure 2 shows the XRD analysis, schematic image of brushite unit cell, and crystal growth planes of brushite. The crystal structure complies with JCPDS 72-0713 (Fig. 2a). The crystalline structure of brushite is monoclinic. The unit cell characteristics of the synthesized brushite include a= 0.581 nm, b= 1.519 nm, c= 0.624 nm and β= 116.4 degree. The unit cell volume is about 493 $Å_3$ (Fig. 2b). The (020) planes with d- spacing of 0.76 nm show one of the preferred growth directions (Fig. 2c) [28].

Probably due to high pressure and high temperature, all of the primary brushite is dissolved in hydrothermal autoclave, and the nucleation and growth process of hydroxyapatite is performed.

Figure 3 shows the XRD analysis, schematic image of hydroxyapatite unit cell, and crystal growth planes of hydroxyapatite. The crystal structure complies with JCPDS 09-0432 (Fig. 3a). The crystalline structure of HA is hexagonal. The unit cell characteristics of the synthesized HA include a= 0.94 nm and c= 0.69 nm. The unit cell volume is about 530 $Å_3$ (Fig. 3b). The (002) planes with d- spacing of 0.34 nm show one of the preferred growth directions (Fig. 3c) [29, 30].

In fact, structural change has not happened. The first structure completely dissolves and disappears and the second structure is synthesized. These structures actually show the thermodynamic equilibrium of each of the calcium phosphates.

Figure 4 shows Raman and FTIR analyzes for powders in two states (Brushite and HA). In both analyzes, synthesis of brushite and HA are confirmed and this analysis together with the ICP analysis results confirm the successful synthesis of hydroxyapatite. Low-intensity, broad and sharp peaks at 428 and 962 cm^{-1}, due to the O-P-O bending mode and the P-O stretching mode of PO_4 groups respectively (symmetric stretching of tetrahedral oxygen atoms around phosphorus atoms), only are revealed in the HA phase with high crystallinity. The peak at 1049 cm^{-1} refers to apatite phosphate groups only visible in high-quality, stoichiometric HA with high crystallinity (Fig. 4a). Table 1 shows the results of FTIR analysis as shown in Fig. 4b. These findings indicate that the powders contain pure HA [29, 30].

Table 1: The results of FTIR analysis

Wavenumber (cm^{-1})	Bond	Mode
3400- 3500	O-H	Stretching vibration
1095	P-O(H)	Stretching vibration
1035	P-O(H)	Stretching vibration
925	P-O(H)	Stretching vibration
565	P-O	Bending

Figure 5 shows the microscopic images of the synthesized hydroxyapatite. The particle morphology is in the form of nanorods. The rods diameter is about 35 nm and their length varies from 50 to 250 nm. The direction of particle growth is <002> and some agglomeration is observed in the final synthesized samples. It can be seen, the diameters of the particles are uniform throughout, indicating a high crystallinity of the particles [29, 30].

Figure 6 shows the microscopic images (TEM) of the synthesized hydroxyapatite. The results of this analysis confirm the information in FESEM images. The sharpness of the particles tip in these images shows that the crystallinity of the particles is extremely high. The preferred growth orientation is C axis [29, 30].

Figure 7 shows the HRTEM image, FFT, and IFFT analysis of the synthesized hydroxyapatite. This analysis proves that the main crystals growth direction in synthesized hydroxyapatite is <002> (C axis). The d- spacing between the specified planes is 0.34 nm [29, 30].

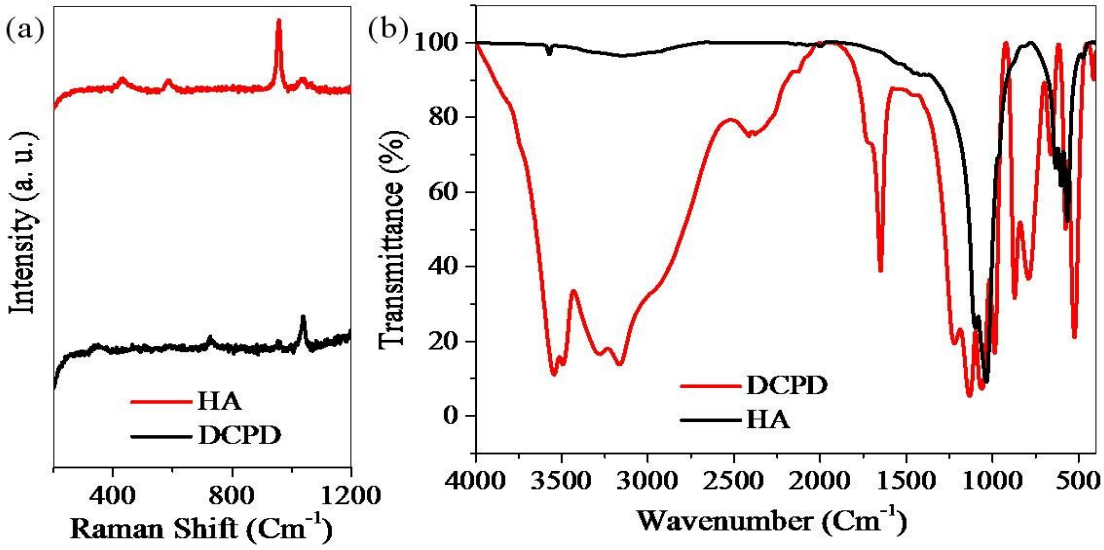

Figure 4: Raman (a) and FTIR (b) analyzes for powders in two states.

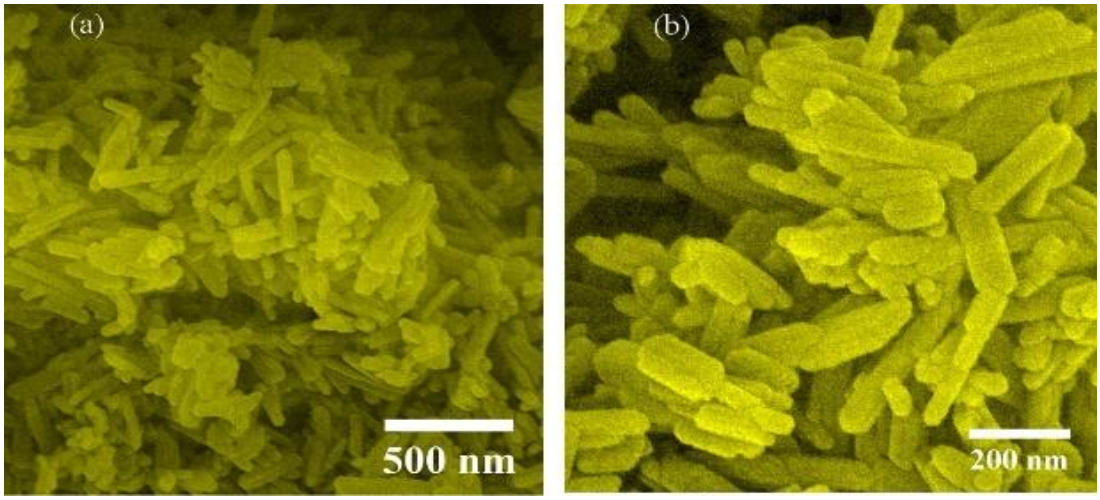

Figure 5: The microscopic images (FESEM) of the synthesized hydroxyapatite.

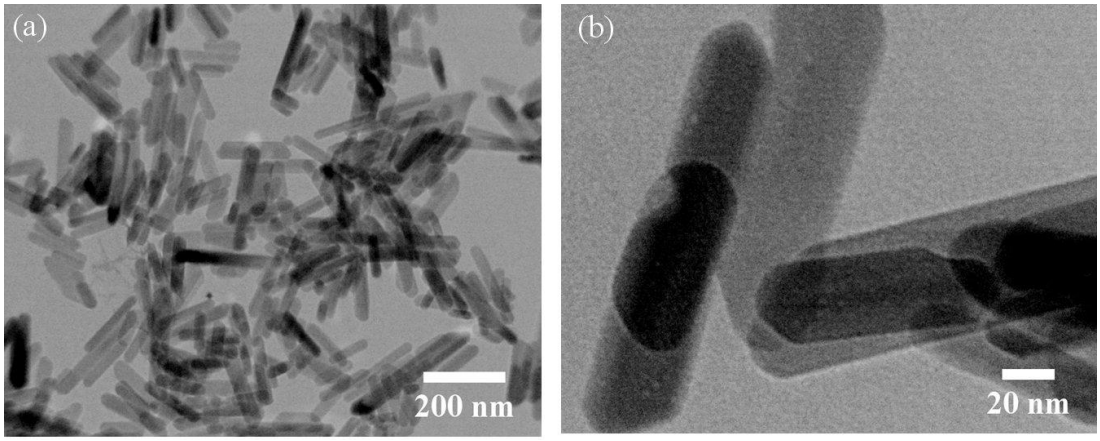

Figure 6: the microscopic images (TEM) of the synthesized hydroxyapatite.

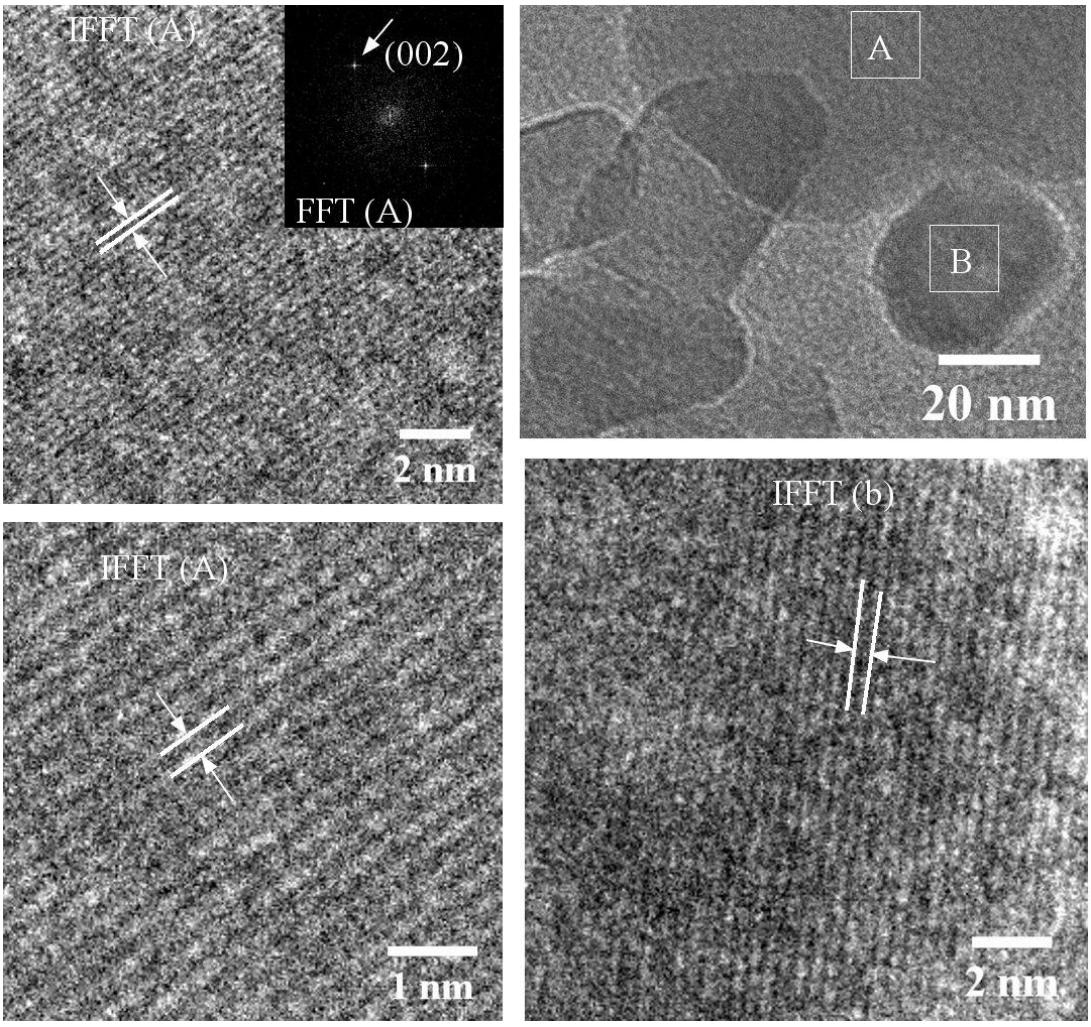

Figure 7: The HRTEM image, FFT, and IFFT analysis of the synthesized hydroxyapatite.

4. Conclusion

The results of this study showed that the initial brushite used in the hydrothermal process was dissolved, followed by the nucleation process and the growth of hydroxyapatite. The synthesized powders in this study were rod-shaped, with 35 nm in diameter and between 50 and 250 nm in length. The main direction of rod growth was <002>, which is C axis. The powders synthesized in this research have the potential to be used in bone tissue engineering, implantation, and drug delivery.

Conflict of interest

The authors certify that they have no affiliations with or involvement in any organization or entity with any financial interest, or non-financial interest in the subject matter or materials discussed in this manuscript.

Acknowledgements

Not applicable.

References

[1] D.E. Aston, J.R. Bow, D.N. Gangadean, Mechanical properties of selected nanostructured materials and complex bio-nano, hybrid and hierarchical systems, Int.

[2] Mater. Rev. 58 (2013) 167–202, http://dx.doi.org/10.1179/1743280412Y.0000000012. R.K. Roeder, G.L. Converse, R.J. Kane, W. Yue,

Hydroxyapatite-reinforced polymer biocomposites for synthetic bone substitutes, JOM 60 (2008) 38–45.

[3] F. Munarin, P. Petrini, R. Gentilini, R.S. Pillai, S. Dirè, M.C. Tanzi, V.M. Sglavo, Microand nano-hydroxyapatite as active reinforcement for soft biocomposites, Int. J. Biol. Macromol. 72 (2015) 199–209, http://dx.doi.org/10.1016/j.ijbiomac.2014.07.050.

[4] Z. Fang, Q. Feng, Improved mechanical properties of hydroxyapatite whiskerreinforced poly(l-lactic acid) scaffold by surface modification of hydroxyapatite, Mater. Sci. Eng. C 35 (2014) 190–194, http://dx.doi.org/10.1016/j.msec.2013.11.008.

[5] V. Uskoković, D.P. Uskoković, Nanosized hydroxyapatite and other calcium phosphates: chemistry of formation and application as drug and gene delivery agents, J. Biomed. Mater. Res. B Appl. Biomater. 96B (2011) 152–191, http://dx.doi.org/10.1002/jbm.b.31746.

[6] X. Li, Y. Yang, Y. Fan, Q. Feng, F. Cui, F. Watari, Biocomposites reinforced by fibers or tubes as scaffolds for tissue engineering or regenerative medicine: biocomposites reinforced by fibers or tubes, J. Biomed. Mater. Res. A 102 (2014) 1580–1594, http://dx.doi.org/10.1002/jbm.a.34801.

[7] T. Liu, X. Ding, D. Lai, Y. Chen, R. Zhang, J. Chen, X. Feng, X. Chen, X. Yang, R. Zhao, K. Chen, X. Kong, Enhancing in vitro bioactivity and in vivo osteogenesis of organic–inorganic nanofibrous biocomposites with novel bioceramics, J. Mater. Chem. B 2 (2014) 6293, http://dx.doi.org/10.1039/C4TB00889H.

[8] C.Z. Liao, K. Li, H.M.Wong, W.Y. Tong, K.W.K. Yeung, S.C. Tjong, Novel polypropylene biocomposites reinforced with carbon nanotubes and hydroxyapatite nanorods for bone replacements, Mater. Sci. Eng. C 33 (2013) 1380–1388, http://dx.doi.org/10.1016/j.msec.2012.12.039.

[9] C. Wan, B. Chen, Poly(ε-caprolactone)/graphene oxide biocomposites: mechanical properties and bioactivity, Biomed. Mater. 6 (2011) 055010, http://dx.doi.org/10.1088/1748-6041/6/5/055010.

[10] P. Wang, L. Zhao, J. Liu, M.D. Weir, X. Zhou, H.H.K. Xu, Bone tissue engineering via nanostructured calcium phosphate biomaterials and stem cells, Bone Res. 2 (2014) 14017, http://dx.doi.org/10.1038/boneres.2014.17.

[11] D.S.H. Lee, Y. Pai, S. Chang, D.H. Kim, Microstructure, physical properties, and bone regeneration effect of the nano-sized β-tricalcium phosphate granules, Mater. Sci. Eng. C 58 (2016) 971–976, http://dx.doi.org/10.1016/j.msec.2015.09.047.

[12] F. Peng, X. Yu, M. Wei, In vitro cell performance on hydroxyapatite particles/poly(Llactic acid) nanofibrous scaffolds with an excellent particle along nanofiber orientation, Acta Biomater. 7 (2011) 2585–2592, http://dx.doi.org/10.1016/j.actbio.2011.02.021.

[13] Y. Deng, H.Wang, L. Zhang, Y. Li, S. Wei, In situ synthesis and in vitro biocompatibility of needle-like nano-hydroxyapatite in agar–gelatin co-hydrogel, Mater. Lett. 104 (2013) 8–12, http://dx.doi.org/10.1016/j.matlet.2013.03.145.

[14] M. Jevtić, M. Mitrić, S. Škapin, B. Jančar, N. Ignjatović, D. Uskoković, Crystal structure of hydroxyapatite nanorods synthesized by Sonochemical homogeneous precipitation, Cryst. Growth Des. 8 (2008) 2217–2222, http://dx.doi.org/10.1021/cg7007304.

[15] D.O. Costa, S.J. Dixon, A.S. Rizkalla, One- and three-dimensional growth of hydroxyapatite nanowires during sol–gel–hydrothermal synthesis, ACS Appl. Mater. Interfaces 4 (2012) 1490–1499, http://dx.doi.org/10.1021/am201735k.

[16] Q. Sun, J.-T. Lou, F. Kang, J.-F. Chen, J.-X.Wang, Facile preparation of hydroxyapatite nanotubes assisted by needle-like calcium carbonate, Powder Technol. 261 (2014) 49–54, http://dx.doi.org/10.1016/j.powtec.2014.04.014.

[17] B.B. Chandanshive, P. Rai, A.L. Rossi, O. Ersen, D. Khushalani, Synthesis of hydroxyapatite nanotubes for biomedical applications,Mater. Sci. Eng. C 33 (2013) 2981–2986, http://dx.doi.org/10.1016/j.msec.2013.03.022.

[18] Y. Zhang, J. Lu, J. Wang, S. Yang, Y. Chen, Synthesis of nanorod and needle-like hydroxyapatite crystal and role of pH adjustment, J. Cryst. Growth 311 (2009) 4740–4746, http://dx.doi.org/10.1016/j.jcrysgro.2009.09.018.

[19] L. Xia, K. Lin, X. Jiang, B. Fang, Y. Xu, J. Liu, D. Zeng, M. Zhang, X. Zhang, J. Chang, Z. Zhang, Effect of nano-structured bioceramic surface on osteogenic differentiation of adipose derived stem cells, Biomaterials 35 (2014) 8514–8527, http://dx.doi.org/10.1016/j.biomaterials.2014.06.028.

[20] B.-Q. Lu, Y.-J. Zhu, F. Chen, C. Qi, X.-Y. Zhao, J. Zhao, Solvothermal transformation of calcium oleate precursor into large-sized highly ordered arrays of ultralong hydroxyapatite Microtubes, Chem. Eur. J. (2014) 1–7, http://dx.doi.org/10.1002/chem.201400252.

[21] B. Jokić, M. Mitrić, V. Radmilović, S. Drmanić, R. Petrović, D. Janaćković, Synthesis and characterization ofmonetite and hydroxyapatite whiskers obtained by a hydrothermal method, Ceram. Int. 37 (2011) 167–173, http://dx.doi.org/10.1016/j.ceramint.2010.08.032.

[22] X. Guo, L. Yu, L. Chen, H. Zhang, L. Peng, X. Guo,W. Ding, Organoamine-assisted biomimetic synthesis of faceted hexagonal hydroxyapatite nanotubes with prominent stimulation activity for osteoblast proliferation, J. Mater. Chem. B 2 (2014) 1760, http://dx.doi.org/10.1039/c3tb21652g.

[24] I.S. Neira, Y.V. Kolen'ko, O.I. Lebedev, G. Van Tendeloo, H.S. Gupta, F. Guitián, M. Yoshimura, An effective morphology control of hydroxyapatite crystals via hydrothermal synthesis, Cryst. Growth Des. 9 (2008) 466–474.

[25] F.Mohandes,M. Salavati-Niasari, Particle size and shapemodification of hydroxyapatite nanostructures synthesized via a complexing agent-assisted route, Mater. Sci. Eng. C 40 (2014) 288–298, http://dx.doi.org/10.1016/j.msec.2014.04.008.

[26] F. Mohandes, M. Salavati-Niasari, Z. Fereshteh, M. Fathi, Novel preparation of hydroxyapatite nanoparticles and nanorods with the aid of complexing agents, Ceram. Int. 40 (2014) 12227–12233, http://dx.doi.org/10.1016/j.ceramint.2014.04.066.

[27] F. Mohandes, M. Salavati-Niasari, Simple morphology-controlled fabrication of hydroxyapatite nanostructures with the aid of new organic modifiers, Chem. Eng. J. 252 (2014) 173–184,

[23] M.-G.Ma, Y.-J. Zhu, J. Chang, Monetite formed inmixed solvents of water and ethylene glycol and its transformation to hydroxyapatite, J. Phys. Chem. B 110 (2006) 14226–14230, http://dx.doi.org/10.1021/jp061738r.

http://dx.doi.org/10.1016/j.cej.2014.05.026.

[28] H. Nosrati, D. Q. S. Le, R. Z. Emameh, C. E. Bunger, Characterization of the Precipitated Dicalcium Phosphate Dehydrate on the Graphene Oxide Surface as a Bone Cement Reinforcement, Journal of Tissues and Materials, 2(1), (2019) 33-46, DOI: 10.22034/jtm.2019.173565.1013.

[29] H. Nosrati, R. Sarraf Mamoory, F. Dabir, M. Canillas Perez, M. A. Rodriguez, D. Q. Svend Le, C. E. Bunger, In situ synthesis of three dimensional graphene-hydroxyapatite nano powders via hydrothermal process, Materials Chemistry and Physics, 222, (2019) 251–255, https://doi.org/10.1016/j.matchemphys.2018.10.023

[30] H. Nosrati, R. Sarraf Mamoory, F. Dabir, D. Q. Svend Le, C. E. Bunger, M. Canillas Perez, M. A. Rodriguez, Effects of hydrothermal pressure on in situ synthesis of 3D graphene/hydroxyapatite nano structured powders, Ceramics International, 45, (2019) 1761–1769, https://doi.org/10.1016/j.ceramint.2018.10.059